Science Advances
AAAS

advances.sciencemag.org/cgi/content/full/5/10/eaaw5841/DC1

Supplementary Materials for

Low-temperature synthesis of polycyclic aromatic hydrocarbons in Titan's surface ices and on airless bodies

Matthew J. Abplanalp, Robert Frigge, Ralf I. Kaiser*

*Corresponding author. Email: ralfk@hawaii.edu

Published 16 October 2019, *Sci. Adv.* **5**, eaaw5841 (2019)
DOI: 10.1126/sciadv.aaw5841

This PDF file includes:

Supplementary Text

Galactic Cosmic Rays. Galactic cosmic rays (GCRs) penetrating Titan's dense atmosphere produce secondary electrons. Here, energetic electrons (5 keV) were employed to mimic the secondary electrons formed in the track of GCRs, a validated approach to mimic the chemical processing of ices via GCRs (*66*). The dose transferred to the ice from each electron (D) in the experiment can be calculated via CASINO simulations by accounting for the initial energy of each electron (E_i), back scattered electron energy (E_{bs}), transmitted electron energy (E_{tr}), and the fraction of electrons that were back scattered or transmitted (f_{bs}/f_{tr}) (table S3; equation [1])

$$D = E_i - (E_{bs} \times f_{bs}) - (E_{tr} \times f_{tr}) \qquad [1]$$

The dose imparted by each electron on average was calculated to be 4000 eV electron^{-1}, and operating the electron gun at a current of 30 nA for 45 minutes generates 5.1×10^{14} electrons; resulting in a fluence of 2.0×10^{18} eV cm^{-2} delivered to the acetylene ice as the substrate is 1 cm^{-2}. Several groups have calculated the GCR flux to Titan's surface resulting in a range of values from $6.2 \times 10^{8} – 6.2 \times 10^{9}$ eV cm^{-2} s^{-1} (*15, 36, 37*). Using the higher and lower bounds of these values the experimental fluence corresponds to 10.4 – 104 years, respectively, of exposure time for acetylene ice on Titan's surface.

Yields. In order to determine the yields of benzene, phenylacetylene, styrene, naphthalene, and phenanthrene a calibration factor for the ReTOF-MS signal must be obtained. First, calibration ices of pure methylacetylene (C_3H_4; Organic Technologies, 99%), propene (C_3H_6; Aldrich, ≥ 99%), 1,3-butadiene (C_4H_6; Aldrich, ≥ 99%), and a mixed ice of 1% methylacetylene, 1% propene, and 1% 1,3-butadiene in methane were deposited onto the substrate with thicknesses of 650 ± 50 nm measured via laser interferometry utilizing refractive indices of 1.38, 1.32, 1.39 for methylacetylene, propene, and 1,3-butadiene, respectively. The thickness for each ice layer and the corresponding densities ($\rho_{methylacetylene}$ = 0.89 g cm^{-3}, $\rho_{propene}$ = 0.80 g cm^{-3}, $\rho_{1,3\text{-butadiene}}$ = 0.97 g cm^{-3}) (*67*) were then used to determine the number of molecules present in each calibration ice via a modified Beer-Lambert relationship (*68*). Next, by monitoring these calibration hydro-carbons during sublimation via PI-ReTOF-MS (PI = 10.49 eV) the number of integrated counts (A_{ReTOF}), corrected for flux (F) and the photoionization cross section (σ) from each molecule can be correlated to the number of molecules of each hydrocarbon determined to be in the ice (γ),

which results in a PI-ReTOF-MS calibration factor (α) of $(2.71 \pm 0.76) \times 10^{12}$ molecules cm^2 integrated $counts^{-1}$ (*69*) (equation [2])

$$\alpha = \gamma \times \sigma \times (A_{ReTOF} \times F)^{-1} \quad [2]$$

Using this PI-ReTOF-MS calibration factor and knowing the amount of energy deposited into the ice (2.0×10^{18} eV cm^{-2}) allows for the yield (molecules eV^{-1}) of individual molecules to be determined from only PI-ReTOF-MS counts (table S4). For example, the yield of benzene can be calculated by rearranging equation [2] to solve for the number of benzene molecules ($\gamma_{benzene}$) produced from the irradiated acetylene ice. Since the ion signal for *m/z* = 78 from the 1+1 REMPI experiment at λ = 258.994 nm is only due to benzene this signal can be scaled to the same intensity as the *m/z* = 78 signal detected from the SPI experiment at 10.49 eV; this signal was integrated to determine the number of counts due to benzene ($A_{ReTOF\text{-}benzene}$) as the photoionization cross section ($\sigma_{benzene}$) has been determined at 10.49 eV to be 30 ± 6 Mb (*70-74*). Applying the PI-ReTOF-MS calibration factor ($\alpha = (2.71 \pm 0.76) \times 10^{12}$ molecules cm^2 $counts^{-1}$), the sublimation peak area ($A_{ReTOF\text{-}benzene} = (9.25 \pm 1.85) \times 10^4$ counts), and correcting for differences in flux (F = 0.9) equation [2] determined the yield of benzene to be $\gamma_{benzene} = (3.72 \pm 1.28) \times 10^{-3}$ molecules eV^{-1}. This procedure was repeated for each of the molecules isomer-specifically identified from the REMPI experiments calculating yields of $4.66 \pm 1.63 \times 10^{-4}$, $2.74 \pm 0.96 \times 10^{-4}$, $1.58 \pm 0.55 \times 10^{-4}$, and $1.18 \pm 0.41 \times 10^{-5}$ molecules eV^{-1} for phenylacetylene, styrene, naphthalene, and phenanthrene, respectively (table S4).

Higher Molecular Weight PAHs. The 1+1 REMPI experiment at λ = 258.994 nm was designed to isomer-specifically detect if benzene was produced in the acetylene irradiated ice, but ion signals up to *m/z* = 260 were also detected (table S2, figs. S5 & S6). Interestingly, most ring-carrying aromatics and PAHs have a relatively broad electronic transition in this wavelength regime, and multi-photon ionization experiments are commonly carried out at λ = 248-266 nm to detect trace amounts of PAHs (*75-77*). Table S2 summarizes ion signals detected with possible molecular formulae and related isomers. Here, an interesting trend detected is that the molecular formulae containing an odd numbers of carbon atoms (C_n, n = 9, 11, 13, 15) are consistently related to weaker ion signals than molecular formulae containing an even numbers of carbon atoms (C_n, n = 6, 8, 10, 12, 14, 16) (figs. S5 & S6). Specifically, ion signals corresponding to

PAHs with four six membered rings, such as pyrene ($C_{16}H_{10}^{+}$, *m/z* = 202), were recorded as well as alkylated naphthalenes (methylnaphthalene, $C_{11}H_{10}^{+}$, *m/z* = 142; ethylnaphthalene, $C_{12}H_{12}^{+}$, *m/z* = 156), and alkylated phenanthrenes (methylphenanthrene, $C_{15}H_{12}^{+}$, *m/z* = 192; ethylphenanthrene, $C_{16}H_{14}^{+}$, *m/z* = 206) similar to the pattern observed for the alkylation of the benzene molecule. Other signals detected possibly include indene ($C_9H_8^{+}$, *m/z* = 116) which carrier a six and one five-membered ring, acenaphthene ($C_{12}H_{10}^{+}$, *m/z* = 154) carrying two six and one five-membered ring, and their alkylated relatives methylindene ($C_{10}H_{10}^{+}$, *m/z* = 130), ethylindene ($C_{11}H_{12}^{+}$, *m/z* = 144), methyacenaphthene ($C_{13}H_{12}^{+}$, *m/z* = 168), and ethylacephthene ($C_{14}H_{14}^{+}$, *m/z* = 182). However, these ion signals have multiple possible isomers and assignments will need individual confirmation experiments to be definitive in their isomer-specific identification, but these signals can only belong to ring-carrying aromatics and PAHs produced from the irradiated acetylene ice.

Table S1. Infrared absorption features recorded before and after the irradiation of acetylene (C2H2) and D2-acetylene (C2D2) ices at 5 K.

Absorptions Before Irradiation (cm^{-1})	Absorptions After Irradiation (cm^{-1})	Assignment	Carrier	References
4076, 3948, 3863		$\nu_1 + \nu_5$, $2\nu_2$, $\nu_2 + 2\nu_4 + \nu_5$ (C_2H_2)	Combination/ Overtone	(*25*)
3328		ν_1 (C_2H_2)	CH stretch	(*25*)
	3320	ν_4 (C_4H_2)	CH stretch	(*78*)
	3280	ν_1 (C_4H_4)/ν_{CH} (R-C≡CH)	CH stretch	(*17, 79, 80*)
3235		ν_3 (C_2H_2)	CH stretch	(*25*)
	3154	ν_{CH} (R-$CHCH_2$)	CH_2 asymmetric stretch	(*17, 18*)
	3094	ν_9 (C_2H_4)	CH_2 asymmetric stretch	(*81*)
	*3030	ν_3 (C_4H_4)/ ν_8+ν_{19} (C_6H_6)/ν_{CH} (Aromatic)	=CH stretch/Combination/Aromatic CH stretch	(*18, 19, 27, 82-84*)
3005		ν_3 ($^{13}C_2H_2$)	CH stretch	(*25*)
	2974	ν_{10} (C_2H_6)/ν_{11} (C_2H_4)/ν_6 + ν_7 (C_4H_4)	CH_3 degenerate stretch/CH_2 symmetric stretch/combination	(*17, 81*)
	2884	ν_5 (C_2H_6)	CH_3 symmetric stretch	(*85*)
2735, 2708		$\nu_2 + \nu_5$ (C_2H_2)	Combination	(*86, 87*)
2545		ν_3 (C_2DH)	CD stretch	(*86*)
	2090	ν (C≡C≡C)	Asymmetric stretch	(*88*)
1961		ν_2 (C_2H_2)	C≡C stretch	(*87*)
	1951	ν (C=C=C)	Asymmetric stretch in RCH=C=CH_2	(*17*)
	1600	ν_6 (C_4H_4)	C=C stretch	(*17, 80, 89*)
1389		$\nu_4 + \nu_5$ (C_2H_2)	Combination	(*86*)
	1240	$2\nu_{17}$ (C_4H_4)/$\nu_6 + \nu_8$ (C_4H_2)	Overtone/Combination	(*17, 78, 80, 87*)
	*1010-890	ν_{20} (C_6H_6)/ν_{CH} (Aromatic)	Out-of-plane CH deformation modes in substituted benzenes and PAHs	(*19, 21, 79, 82, 83, 90, 91*)
741		ν_5 (C_2H_2)	CCH bend	(*25*)
	690	ν_{11} (C_6H_6)	CH bend	(*17*)
C_2D_2 assignments				
5015		$\nu_1 + \nu_3$ (C_2D_2)	Combinations	(*86*)
3278		$\nu_1 + \nu_5$ (C_2D_2)	Combinations	(*86*)
3244		ν_3 (C_2H_2)	CH stretch	(*25*)
2925		$\nu_3 + \nu_4$ (C_2D_2)	Combination	(*86*)
2680		ν_1 (C_2D_2)	CD stretch	(*86*)
	2573	ν_4 (C_4D_2)/ν_4 (C_4D_4)	CD stretch	(*92, 93*)
2544		ν_3 (C_2DH)	CD stretch	(*86*)
2400		ν_3 (C_2D_2)	CD stretch	(*86*)
2341		ν_3 ($^{13}C_2D_2$)	CD stretch	(*86*)
	2335	ν_9 (C_2D_4)	CD_2 asymmetric stretch	(*81*)
2320		$\nu_2 + \nu_5$ (C_2D_2)	Combination	(*86*)
	*2265	ν_{18} (C_6D_6)/ν_{CD} (Aromatic)	CH stretch/ Aromatic CH stretch	(*20, 22, 23, 89, 94*)
	2230	ν_{10} (C_2D_6)	CD_3 degenerate stretch	(*95*)
	2192	ν_{11} (C_2D_4)	CD_2 symmetric stretch	(*81*)
1101		$2\nu_5$ (C_2D_2)	Overtone	(*86*)
1085		$\nu_4 + \nu_5$ (C_2D_2)	Combination	(*86*)
	*800-750	ν_{CD} (Aromatic)	Out-of-plane CH deformation modes in substituted benzenes and PAHs	(*20-23*)
717		ν_5 (C_2H_2)	CH bend	(*86*)
579		ν_5 (C_2D_2)	CD bend	(*86*)

**Notes: ***designates vibrations possibly related to polycyclic aromatic hydrocarbons.

Table S2. Ion signal detected during [1+1] REMPI at λ = 258.994 nm.		
m/z	**Molecular formula***	**Possible PAH Assignment**
78	C_6H_6	Benzene
92	C_7H_8	Toluene
102	C_8H_6	Phenylacetylene
104	C_8H_8	Styrene
106	C_8H_{10}	Ethylbenzene, Dimethylbenzene, Xylene
116	$\mathit{C_9H_8}$	Indene, 1-Propynylbenzene, Methylphenylacetylene
118	$\mathit{C_9H_{10}}$	Indane, Methylstyrene
126	$C_{10}H_6$	Diethynylbenzene, Acepentalene
128	$C_{10}H_8$	Naphthalene
130	$C_{10}H_{10}$	Methylindene, Diethenylbenzene, Dihydronaphthalene
132	$C_{10}H_{12}$	Dihydromethylindene, Diethylbenzene, Tetrahydronaphthalene
140	$\mathit{C_{11}H_8}$	2-Ethynyl-1H-indene, Pentadiynylbenzene
142	$\mathit{C_{11}H_{10}}$	Ethylideneindene, Methylnaphthalene
144	$\mathit{C_{11}H_{12}}$	Ethylindene, Dimethylindene, Dihydromethylnaphthalene
152	$C_{12}H_8$	Acenaphthylene, Biphenylene, Ethynylnaphthalene, Indacene
154	$C_{12}H_{10}$	Biphenyl, Acenaphthalene, Ethenylnaphthalene
156	$C_{12}H_{12}$	Dimethylnaphthalene, Ethylnaphthalene
158	$C_{12}H_{14}$	Trimethyllindene, Phenylcyclohexene
164	$\mathit{C_{13}H_8}$	Fluorenylidene, Heptatriynylbenzene
166	$\mathit{C_{13}H_{10}}$	Fluorene, 1H-Phenalene
168	$\mathit{C_{13}H_{12}}$	Methylacenaphthene methylbiphenyl, dibenzofuran
170	$\mathit{C_{13}H_{14}}$	Trimethylnaphthalene, Propylnaphthalene
176	$\mathit{C_{14}H_8}$	Pyracyclene, Diethynylnaphthalene
178	$C_{14}H_{10}$	Phenanthrene
180	$C_{14}H_{12}$	9,10-Dihydrophenanthrene, Dimethylacenaphthylene
182	$C_{14}H_{14}$	Dimethylacenaphthene, Dimethylbiphenyl
184	$\mathit{C_{14}H_{16}}$	Diethylnaphthalene, Tetramethylnaphthalene
190	$\mathit{C_{15}H_{10}}$	Methylenephenanthrene, Ethynylfluorene,
192	$\mathit{C_{15}H_{12}}$	Methylphenanthrene, Ethylidenefluorene
194	$\mathit{C_{15}H_{14}}$	Trimethylacenaphthylene, 9-Ethylfluorene
196	$\mathit{C_{15}H_{16}}$	Trimethylacenaphthene, Diphenylpropane
202	$\mathit{C_{16}H_{10}}$	Pyrene, Fluoranthene
204	$\mathit{C_{16}H_{12}}$	Phenylnaphthalene, Dihydropyrene
206	$C_{16}H_{14}$	Dimethylphenanthrene, Tetrahydropyrene
208	$C_{16}H_{16}$	Hexahydropyrene, 9-Propyl-9H-fluorene
210	$C_{16}H_{18}$	Diethylbiphenyl, Tetramethylacenaphthene
234	$\mathit{C_{18}H_{18}}$	Retene, Tetramethylphenanthrene
236	$\mathit{C_{18}H_{20}}$	Octahydronaphthacene, 1,4-Diphenylcyclohexane
260	$\mathit{C_{20}H_{20}}$	Diethyldimethylphenanthrene, Dimethylphenyldimethylnaphthalene

**Notes: ***italics represent weakly detected ion signal.

Table S3. Data applied to calculate the irradiation dose per molecule in C_2H_2 and C_2D_2 ices.

	C_2H_2	C_2D_2
initial kinetic energy of the electrons, E_i	5 keV	5 keV
irradiation current, I	30 ± 3 nA	30 ± 2 nA
total number of electrons	$(5.1 \pm 0.5)\times10^{14}$	$(5.1 \pm 0.5)\times10^{14}$
average kinetic energy of backscattered electrons, E_{bs}^*	3.2 ± 0.3 keV	3.2 ± 0.3 keV
fraction of backscattered electrons, f_{bs}^*	0.32 ± 0.03	0.32 ± 0.03
average kinetic energy of transmitted electrons, E_{tr}^*	0.8 ± 0.1 keV	0.5 ± 0.1 keV
fraction of transmitted electrons, f_{tr}^*	0.01 ± 0.01	0.01 ± 0.01
average penetration depth, l^*	370 ± 40 nm	310 ± 30 nm
density of the ice, ρ	0.76 ± 0.08 g cm^{-3}	0.89 ± 0.09 g cm^{-3}
irradiated area, A	1.0 ± 0.1 cm^2	1.0 ± 0.1 cm^2
total number of molecules processed	$(6.4 \pm 0.6)\times10^{17}$	$(6.0 \pm 0.6)\times10^{17}$
dose per acetylene molecule	3.1 ± 0.3 eV	3.4 ± 0.3 eV

Notes: *CASINO output values. Error bars indicate 10 % (SD).

Table S4. Yields of specific isomers detected via REMPI.					
Molecule	**Formula**	**Adiabatic Ionization Energy (eV)**	**Photoionization Cross Section (Mb)**	**Yield (Molecules eV^{-1})**	**References**
Benzene	C_6H_6	9.244 ± 0.001	30 ± 6	$3.72 \pm 1.28 \times 10^{-3}$	(*70-74*)
Phenylacetylene	C_8H_6	8.825 ± 0.001	63 ± 13	$4.66 \pm 1.60 \times 10^{-4}$	(*96*)
Styrene	C_8H_8	8.464 ± 0.001	40 ± 8	$2.74 \pm 0.94 \times 10^{-4}$	(*73, 96*)
Naphthalene	$C_{10}H_8$	8.144 ± 0.001	51 ± 10	$1.58 \pm 0.54 \times 10^{-4}$	(*97*)
Phenanthrene	$C_{14}H_{10}$	7.891 ± 0.001	56 ± 11	$1.18 \pm 0.41 \times 10^{-5}$	(*97*)
Ratio of REMPI Detected Molecules					
Benzene : Phenylacetylene : Styrene : Naphthalene : Phenanthrene			314 ± 126 : 39 ± 16 : 23 ± 9 : 13 ± 5 : 1 ± 0.4		

Notes: The error bars indicate 35 % (SD).

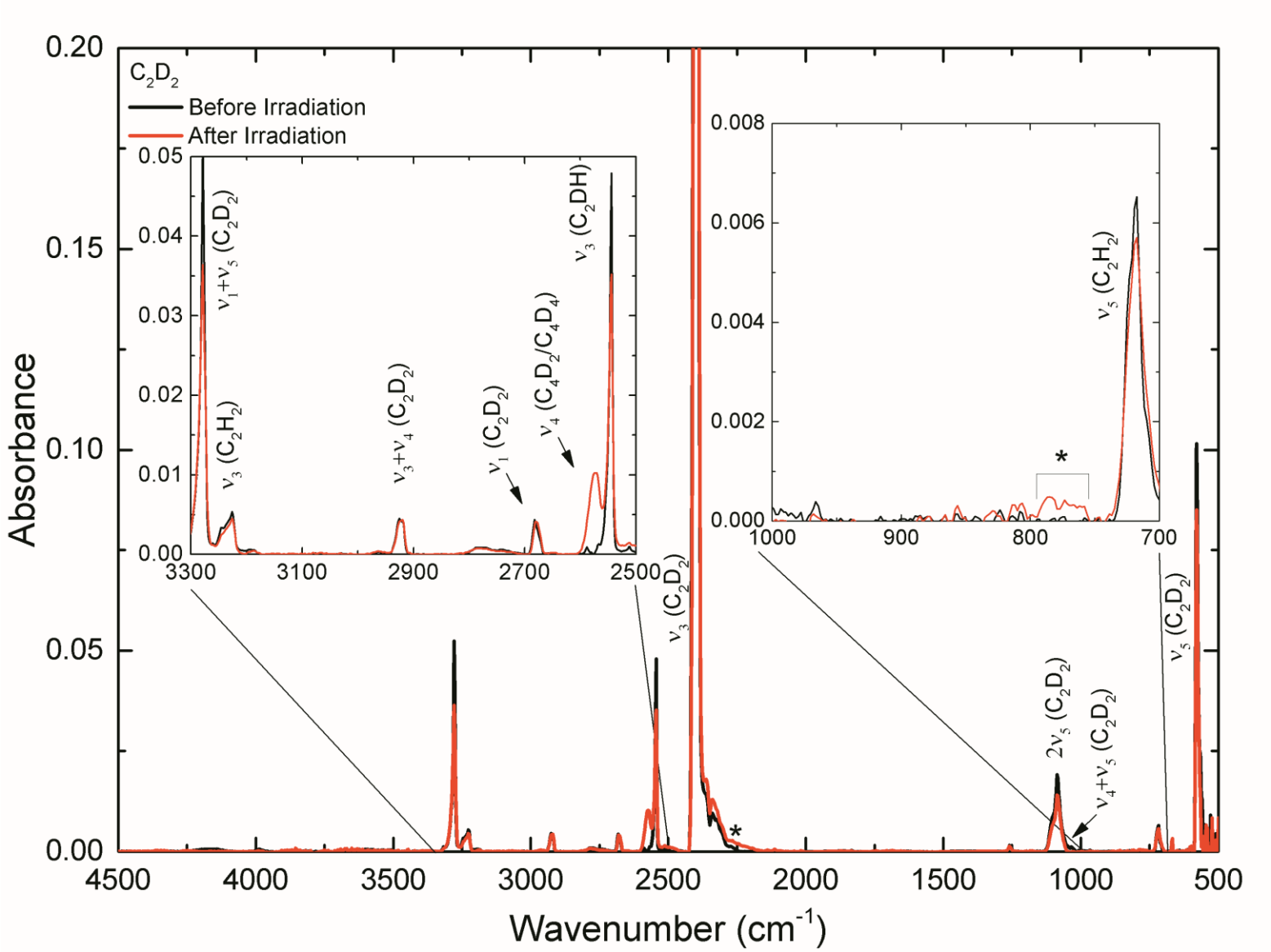

Fig. S1. Deuterated acetylene ice spectra before (black) and after (red) processing with energetic electrons. FTIR spectra from 500-4500 cm^{-1} with PAH related features identified with * (table S2).

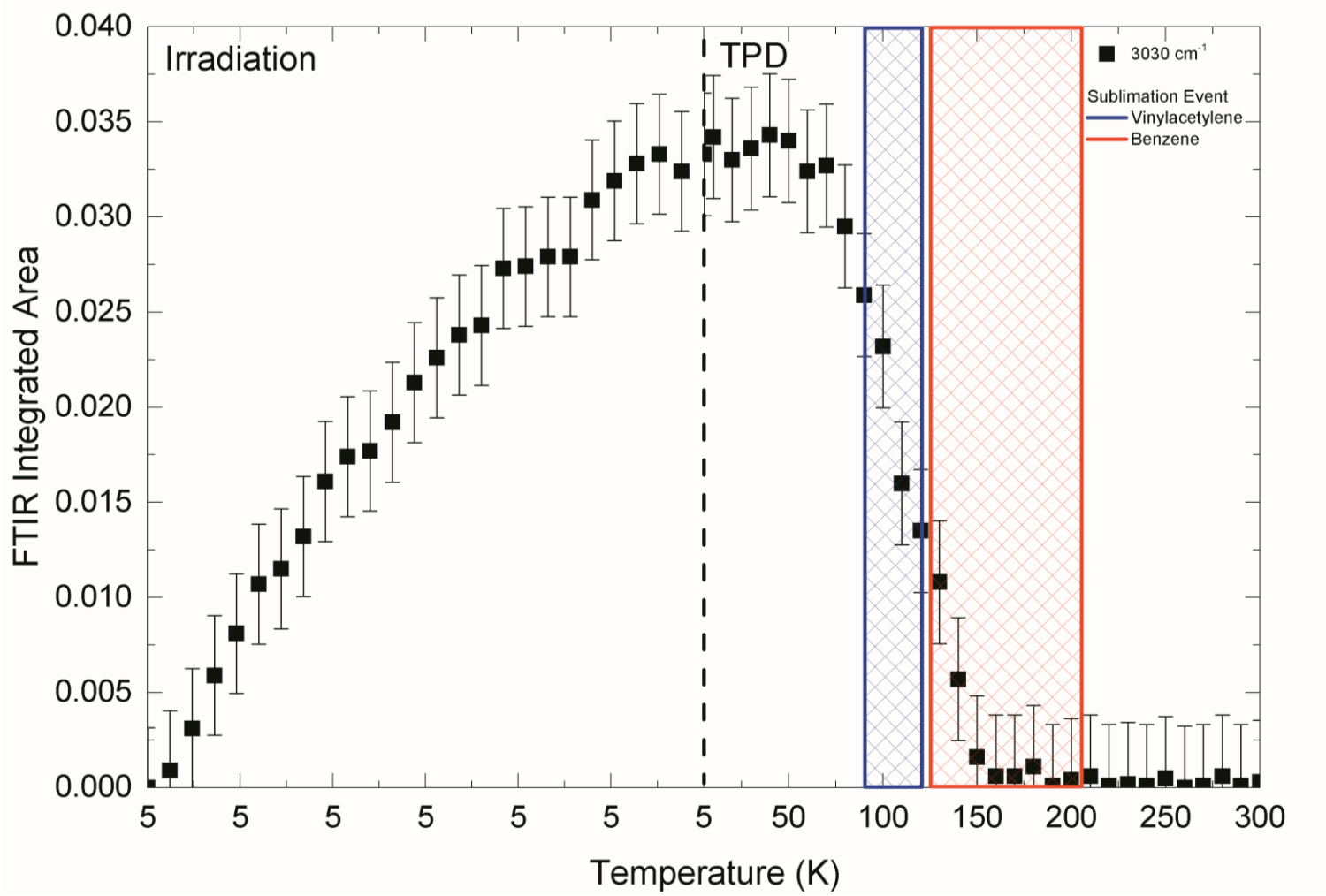

Fig. S2. Temporal profile of the FTIR band at 3030 cm^{-1} during irradiation and TPD. Analysis of the 3030 cm^{-1} feature shows that it only increases in intensity during irradiation and only decreases during TPD corresponding to different possible contributor's sublimation events such as vinylacetylene (blue) and benzene (red). The error bars indicate 10 % (SD).

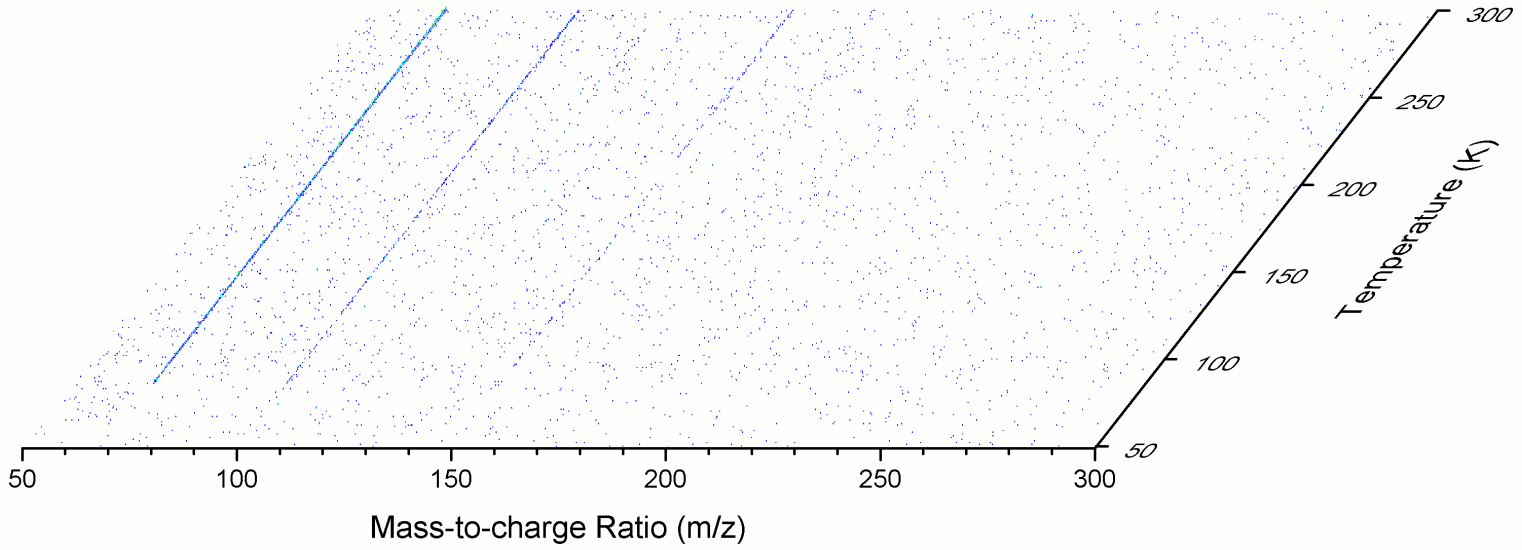

Fig. S3. Temperature-dependent SPI-ReTOF-MS (PI = 10.49 eV) data of the subliming molecules from unirradiated acetylene ice. Three ion signals displayed an intensity slightly above the baseline, but none of these ion counts were connected to mass-to-charge ratios corresponding to benzene, phenylacetylene, styrene, naphthalene, or phenanthrene.

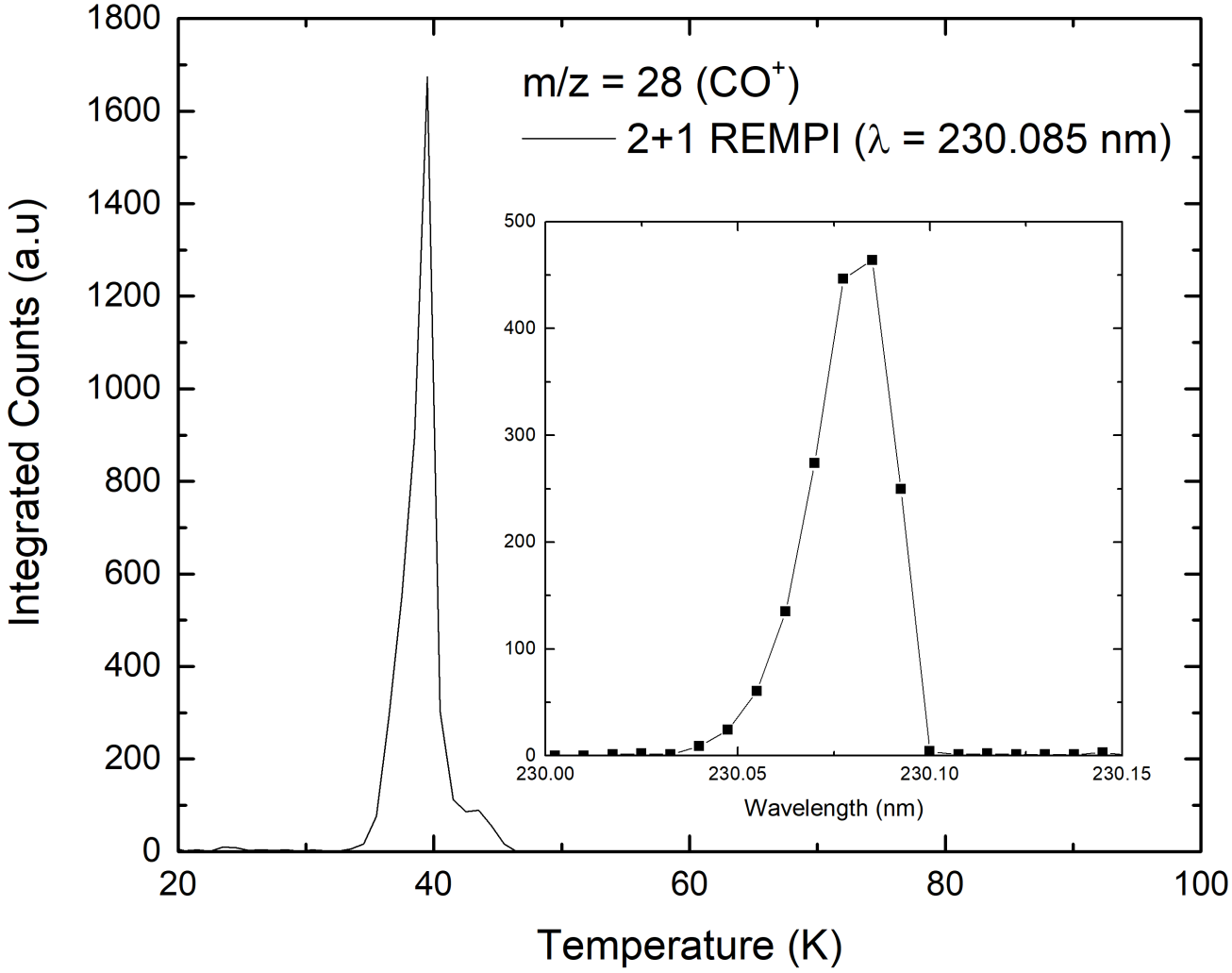

Fig. S4. REMPI-ReTOF-MS spectra versus temperature for carbon monoxide subliming from the substrate used as a calibration compound to confirm the REMPI capabilities of the system. The inset displays the initial scan from 230.00-230.15 nm recorded during sublimation from 38-40 K to determine the wavelength at which the resonance enhanced ionization of carbon monoxide was at a maximum value (λ = 230.085 nm).

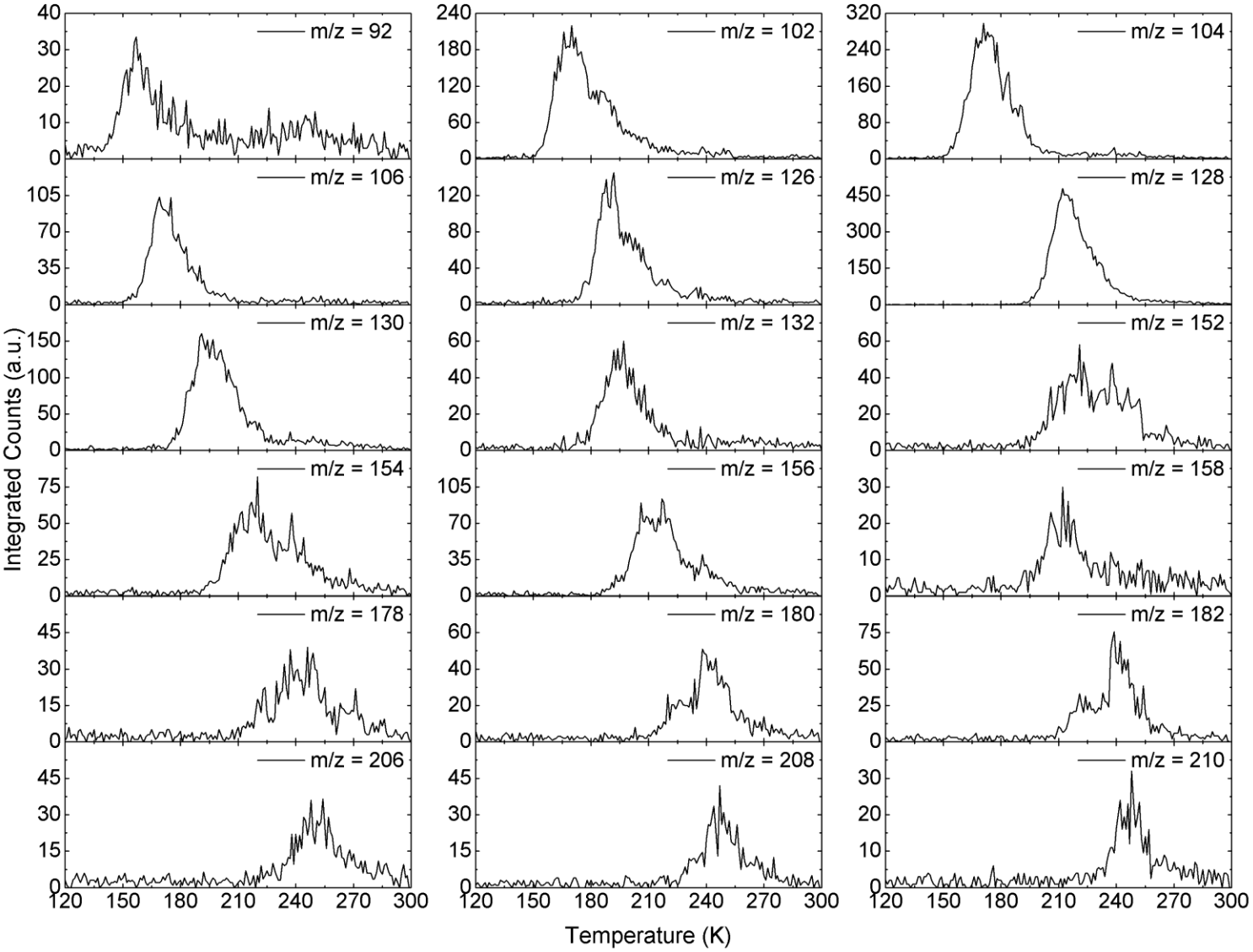

Fig. S5. Dominant ion signals detected during [1+1] REMPI at λ = 258.994 nm. These signals can only be due to aromatic ringed molecules such as PAHs.

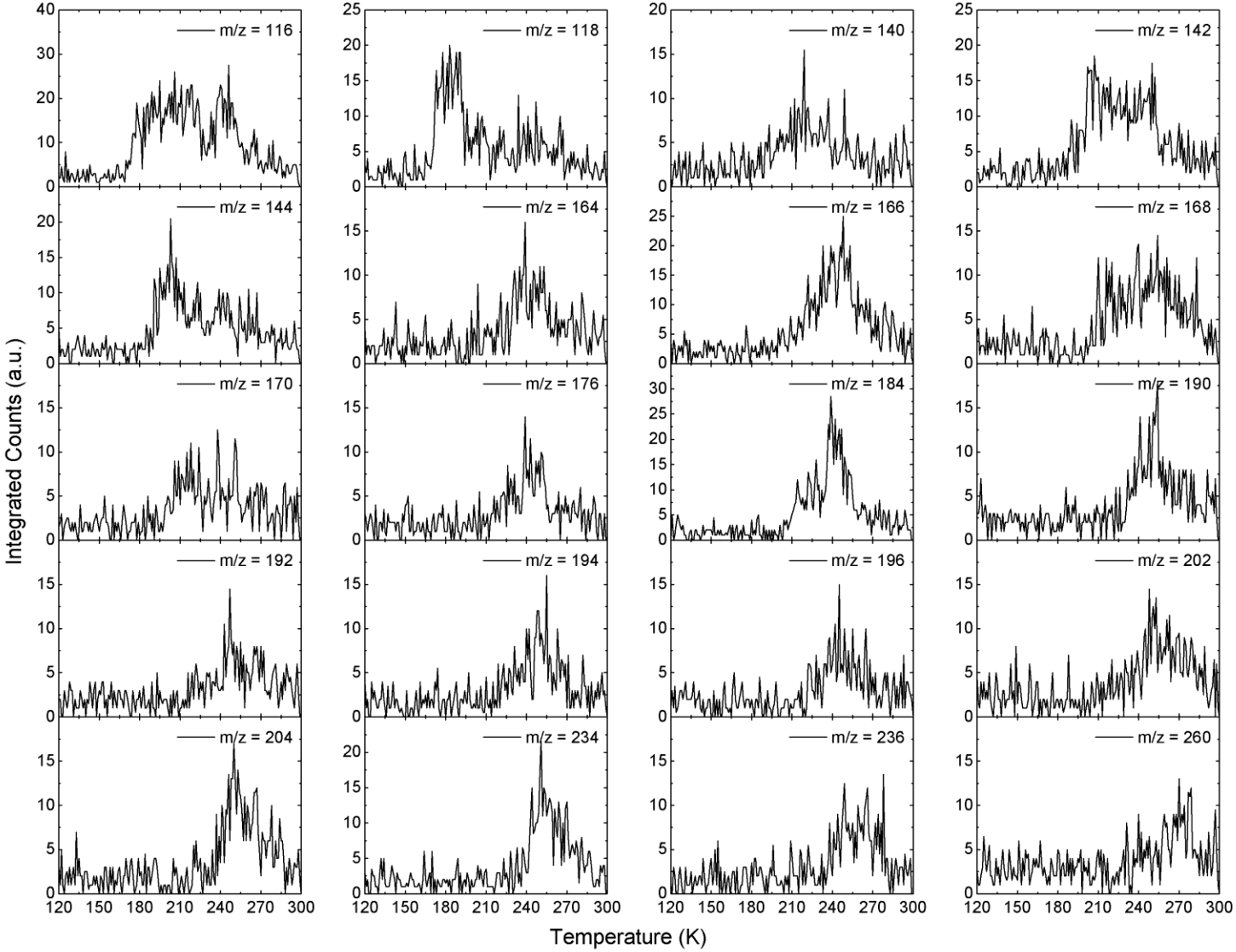

Fig. S6. Weak ion signals detected during [1+1] REMPI at λ = 258.994 nm. These signals can only be due to aromatic ringed molecules such as PAHs